A Magnetic Analyzer for Charged-Particles from Nuclear Reactions

C. W. SNYDER, S. RUBIN, W. A. FOWLER, AND C. C. LAURITSEN
Kellogg Radiation Laboratory, California Institute of Technology, Pasadena 4, California

(Received June 23, 1950)

A double-focusing magnetic spectrometer for detecting and analyzing charged particles from nuclear reactions is described. The magnetic field, varying as $r^{-\frac{1}{2}}$ near an average radius of 10.5 in., extends over a semicircle yielding object and anastigmatic image positions some distance outside of the region of strong field. The acceptance solid angle is $\Omega=0.0061$ sterad. and the momentum resolution with an 8-mm slit at the detector is $R=128$. The ultimate resolution determined by spherical aberration and some residual astigmatism is about 1000. Applications to the study of the energy and yield of nuclear reaction products are discussed.

I. ENERGY ANALYSIS OF NUCLEAR REACTION PRODUCTS

MUCH of our present knowledge of the structure of nuclei has come from an analysis of the kinetic energies of the particles which initiate nuclear reactions or which are produced in nuclear reactions. For some time improved techniques have made possible the production of ion beams which are monoenergetic to a high degree so that detailed features of nuclear structure such as narrow, closely spaced energy levels have become observable through the study of excitation curves of nuclear processes. The equally precise analysis of the kinetic energies or momenta of the products of the reaction is a technique of equal importance which has remained completely unexploited until recently.

A reaction-product analyzer with high dispersion and energy resolution and with large solid angle has several important functions. (1). Under ideal conditions using highly resolved incident particles and thin targets, it makes possible the investigation of fine structure in the groups of particles produced in a reaction and thus of the corresponding fine structure in the energy levels of the residual nuclei. (2). It makes possible the observation of a single group of particles in the presence of a large flux of other particles of greater range. Although "differential" range techniques have been developed, they have not been successful in isolating "weak" short range groups. (3). It makes possible energy measurements of the hitherto neglected "residual nuclei" whose ranges are so short as to be practically unobservable in the usual type of range measurement. This point is particularly important with respect to neutron reactions, the direct determination of fast neutron energies with high precision (<one percent) being impossible at present. This technique has been used by Tollestrup, *et al.*[1] to infer the neutron energy in the reaction $D^2(d, n)He^3$ by analyzing the energy of the He^3. It can also be used to infer the angular distribution and excitation functions of neutrons produced in nuclear reactions. (4). The analyzer can be used with a thin target to study reaction products produced by monoenergetic incident particles even with high energy accelerators which do not produce monoenergetic beams. (5). With monoenergetic incident particles the analyzer is able to pick out charged particles produced in a thin lamina in a thick target, thus making it possible to obtain thin-target data in cases where the actual production of a thin target without backing is not feasible. This technique has been applied to determine the excitation function for elastic scattering of protons in lithium and beryllium. In addition compounds of the element of interest can be employed, the effects of other components being easily avoided. Similarly the effects of surface contaminants can be avoided.[2] (6). The analyzer can be employed for precise measurements of the differential stopping powers of various materials as a function of the energy of the incident particles. The application of such analysis to the determination of differential stopping powers for natural alpha-particles is well known.[3] (7). By the high resolution analysis of elastically scattered particles the analyzer can be used to determine the nuclear composition of thin layers of unknown materials.

II. GENERAL DESCRIPTION OF THE MAGNETIC SPECTROMETER

We have built a magnetic spectrometer[4] and have used it for analyzing the energy of particles produced in several reactions brought about by bombardment with monoenergetic protons and deuterons from an electrostatic accelerator and analyzer previously described.[5] These particles include protons, deuterons, tritons, He^3 nuclei, alpha-particles, Li^6, Li^7, Be^7 and heavier nuclei. For brevity, we shall refer only to protons in the following. The instrument is a modification of the design of Siegbahn and Svartholm[6] for electrons, employing a ring-shaped inhomogeneous magnetic

[1] Tollestrup, Jenkins, Fowler, and Lauritsen, Phys. Rev. **75**, 1947 (1949).

[2] Fowler, Lauritsen, and Rubin, Phys. Rev. **75**, 1471 (1949). Thomas, Rubin, Fowler, and Lauritsen, Phys. Rev. **75**, 1612 (1949).

[3] S. Rosenblum, Ann. d. Physik **10**, 408 (1928).

[4] Snyder, Lauritsen, Fowler, and Rubin, Phys. Rev. **74**, 1564 (1948).

[5] Fowler, Lauritsen, and Lauritsen, Rev. Sci. Inst. **18**, 818 (1947).

[6] K. Siegbahn and N. Svartholm, Arkiv. f. Math. Astron. Fysik. **33A**, No. 21 (1946); N. Svartholm, Arkiv. f. Math. Astron. Fysik. **33A**, No. 24 (1946).

field having the property of double focusing (i.e., anastigmatism). The choice of this instrument over other possible types of analyzers was dictated by two considerations: (1). the difficulty of obtaining fields sufficient to deflect million-volt protons without using iron in the circuit; it is this point which ruled out the "lens type" spectrometer so popular for electrons, and (2). the increased intensity or aperture obtainable with this design in contrast to other types of ferromagnetic spectrometers,[7] when "point" detectors of limited opening are to be employed. It is true that line detectors of sufficient extent can be employed with astigmatic spectrometers but this is often undesirable for other reasons. The high dispersion (twice that of the "180-degree" spectrometer) is also an advantage.

Several double-focusing spectrometers for electrons have been built and the principle has been extensively discussed in recent literature.[7–10] A magnetic field is required which has cylindrical symmetry about a line (the z-axis) and mirror symmetry about a plane which we shall call the "midplane" and designated by $z=0$ in cylindrical coordinates. For an anastigmatic image, the radial component of the field must vanish in the midplane and the axial component must vary as $r^{-\frac{1}{2}}$ in the vicinity of a particular circle $r=r_0$ which we shall designate as the "midcircle." Conjugate foci lie on the midcircle separated by an angular distance of $(2\pi)^{\frac{1}{2}}$ radians or 254.56 degrees.[6] The required magnetic field shape can be obtained by adjusting the contours of the pole faces.

The proton spectrometer, shown in Figs. 1a and 1b differs from that of Siegbahn and Svartholm principally in having the pole pieces cover an angle about the axis of symmetry of only 180° so that the conjugate foci do not lie in the field. It is easily shown that a first-order focus is still obtained in this case although of course some dispersion and resolution for a given solid angle is sacrificed. In studies of prompt nuclear reactions it is advantageous to have the target or source and the reaction product detector in a field free region; for the target this is required in order not to move the incident beam on the target in a variable manner with changing field and for the detector it is important as certain types of detector components such as photomultiplier tubes, etc., do not operate properly in strong fields. The 180-degree angle was chosen in particular so that both pole faces could be machined simultaneously and it also represents a reasonable compromise between the conflicting requirements just discussed. The pole faces were fastened to a half-inch steel plate end-to-end to form a complete circle and were machined on a gap lathe. Pertinent dimensions in inches are as follows: Core: 11.25 in. diameter×6.25 in. height; yoke: 3.00 in. thick×24.0 in. diameter; pole pieces: 24.0 in. o.d.×18.0 in. i.d.; midcircle radius $r_0=10.5$ in. (26.7 cm); and maximum gap: 1.80 in. at $r=11.2$ in.

The magnetic circuit was made in five parts—two pole pieces, two yokes, and the core. For availability reasons, ordinary hot-rolled steel was used and the dimensions are by no means optimum. For example, it would have been preferable to have a core of larger diameter. The coil was designed to take the full output of a 15-kw 120-volt d.c. generator and still be adequately cooled. The seven "pancake coils" were wound individually, each consisting of two layers of 31 turns of No. 7 rectangular (0.091×0.229 in.) double cotton-covered copper wire, the winding being started at the center of the wire so that both leads are at the outside. Wire somewhat thinner and wider would have been preferable, but was not immediately available. Wrapped with 0.007-inch thick cotton tape, varnished and baked, the coils were smooth, rigid, and quite satisfactory. Two single-layer pancakes were wound to go between the ends of the spool and the end cooling plates, but it was decided to use more insulation and dispense with one of them. The inside lead for the half-pancake comes out through a slot in the adjacent cooling plate.

The cylinder and two end plates of the spool were made of steel, $\frac{1}{4}$-in. thick, and threaded for assembly. The cooling plates between the pancakes were cut from $\frac{3}{16}$-in. copper plate. Copper tubing $\frac{5}{16}$ in. in diameter was fitted into channels machined in the plates, flattened to the same thickness as the plates, and soldered in. The cooling plate design can be seen in the horizontal section in Fig. 1a. In assembly, the pancakes were daubed liberally with insulating varnish and separated from the spool and from adjacent cooling plates by a layer of varnished cambric ("empire cloth") 0.012 in. thick. The resistance between the windings or the cooling plates and the spool is in excess of 20 megohms. Water connections to the cooling plates are made with $\frac{1}{4}$-in. "Aeroquip" rubber hose fittings. Water circulates through the plates in parallel, and at 15-kw input the heating is not excessive except on the spool face adjacent to the half-pancake. Continuous operation at currents over 125 amp. is not possible because of the heating of this plate. Cooling plates adjacent to both spool ends should be incorporated. The coil has a resistance of 0.8 ohm and gives approximately 50,000 amp. turns at 15 kw.

The vacuum chamber was made in two half-shells of brass. Two $\frac{7}{8}$-in. plates were bolted side by side on the face plate of a large lathe and the two halves were carved out simultaneously so that they mated exactly. Grooves $\frac{1}{16}$ in. wide and $\frac{1}{16}$ in. deep were machined in the center of the abutting surfaces of the half shells, and these were filled with a tightly fitting brass strip to position the shells as they were soft soldered together. The ends of the box were closed with brass pieces machined to a close fit in the inside of the box and

[7] F. B. Shull and D. M. Dennison, Phys. Rev. **71**, 681 (1947); **72**, 256 (1947); E. S. Rosenblum, *ibid.* **72**, 731L (1947).
[8] F. B. Shull, Phys. Rev. **74**, 917 (1948).
[9] Kurie, Osoba, and Slack, Rev. Sci. Inst. **19**, 771 (1948).
[10] D. Judd, Rev. Sci. Inst. **21**, 213 (1950).

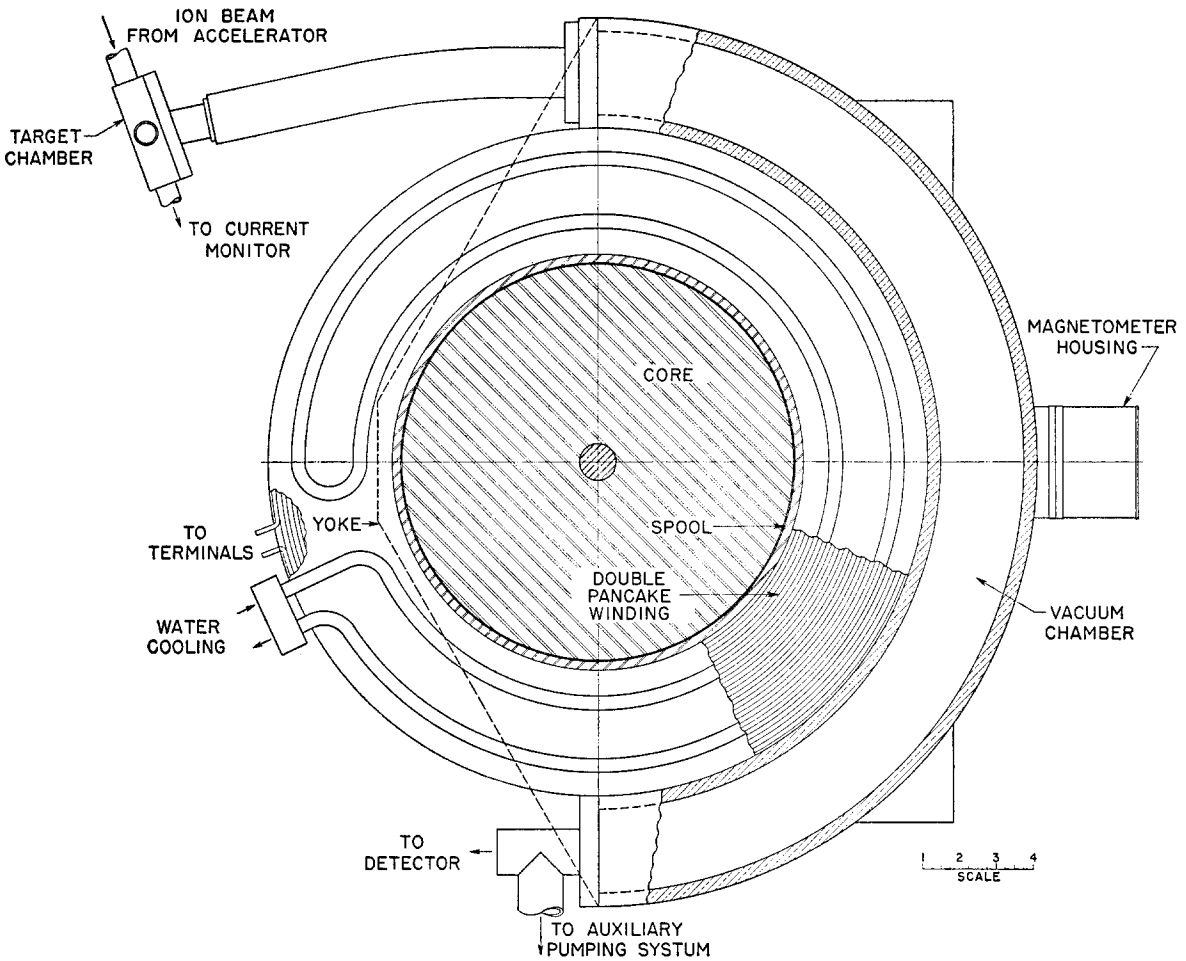

FIG. 1a. Horizontal section of Proton Spectrometer.

soldered in. The box appears to be completely vacuum tight. 0-ring joints are used for connections to the box. The interior cross section is approximately rectangular, $2\frac{1}{4}$ in. wide and $1\frac{1}{2}$ in. high with rounded corners.

The inlet end of the box leading to the target chamber is a length of brass pipe, within which is a short length of brass tubing rotatable about a vertical transverse axis. This aperture stop limits the range of scattering angles accepted by the spectrometer in cases where it is required for precision and is permitted by the intensity. At the exit end of the box, provision is made for attaching a small diffusion pump and liquid air trap. The auxiliary pump and trap are necessitated by the small size of the connections to the main vacuum system.

Shaping of the Magnetic Field

The magnetic field in the midplane can be expressed in the neighborhood of the midcircle in a series of the form[6]

$$H(r)=H_z(r)=H_0\left[1-n\left(\frac{r-r_0}{r_0}\right)+m\left(\frac{r-r_0}{r_0}\right)^2+\cdots\right], \quad (1)$$

where $H_0=H(r_0)$. The double-focusing property requires that $n=\frac{1}{2}$. The values of m and higher order coefficients affect only the aberrations and not the focal length, and they will not be considered here. If n is larger than $\frac{1}{2}$, the r-focal length (i.e., the focal length for trajectories in the midplane with r varying) is longer than the z focal length (i.e., the focal length for trajectories in the cylinder $r=r_0$ with z varying). If n is too small, the reverse is true. In either case the magnetic lens is astigmatic.

The problem of the proper shape of pole face to achieve the field described by $n=\frac{1}{2}$ does not permit of an accurate solution analytically because of the stray field and of non-linearity in the iron. A very simple analysis gives as the first approximation to the slope of the pole pieces at their center the expression

$$\tan u=nz_0/r_0, \quad (2)$$

where u = angle between pole face and midplane; z_0 = coordinate of pole face at $r=r_0$, i.e., half-spacing of pole faces at their center. That this approximation gives the correct answer in the case $n=0$ (parallel faces, uniform field) and the case $n=1$ ($1/r$ field in which equipotentials are coaxial cones with vertices at the origin)

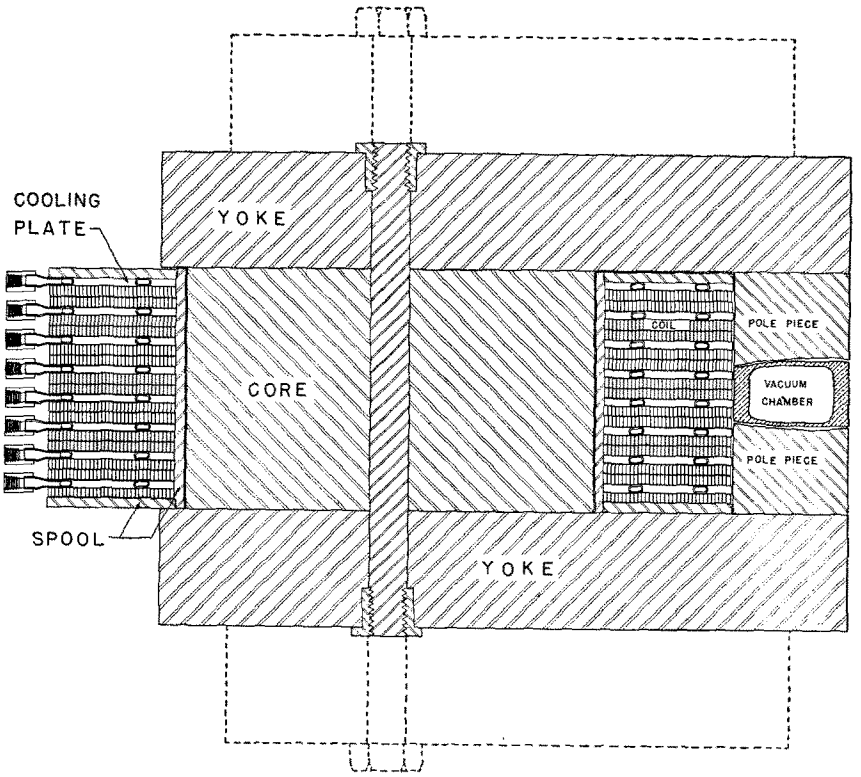

FIG. 1b. Vertical section of Proton Spectrometer.

gives some assurance that it will be valid for the intermediate case $n=\frac{1}{2}$ of interest here. For this spectrometer, it proved to be a good approximation.

Our initial estimate for the proper contour was that shown by the upper curve in Fig. 2. This shape was determined by scaling up the contour published by Siegbahn and Svartholm,[6] but because of slightly altered proportions, the scaling was not exact. The half width of the air gap at its center was 2.20 cm, so that for $n=\frac{1}{2}$ Eq. (2) gives $\tan u=1.10/26.7=0.0412$. Actually $\tan u$ was made equal to 0.0536, and it was expected that this contour might give a field falling off too rapidly with radius and make the z focal length shorter than the r focal length.

Rather than make a detailed investigation of the field shape, the focusing properties were investigated by projecting the proton beam from the electrostatic analyzer directly into the spectrometer and observing the spot produced on a quartz disk at the other end. A small alternating current electromagnet spread the beam in a plane 45 degrees from the vertical so that both radial and vertical focusing effects could be observed. The virtual source in this arrangement is at the center of the magnetic gap. With the source at 36 cm from the end of the pole pieces, the r focus was found to be more than 30 cm beyond the other end and the z focus to be 5 cm inside the gap.

The pole faces were then re-machined to the contour shown in the lower curve of Fig. 2, which was expected to give a slight overcorrection, $\tan u$ being 0.0380, somewhat slightly less than the calculated value 0.0412. Investigation revealed that, for approximately symmetrical cases, the radial focus was now shorter than the vertical focus, but that by moving the source farther away, a very good point image could be obtained. Although a slight improvement in the first-order astigmatism is to be expected from using a larger source than image distance, the improvement observed was considerably greater than that expected and is most certainly to be attributed to second-order effects or to the fringing field. Since the large stray field made it desirable to keep the source well away from the magnet in order to minimize the deflection of the incident beam, this arrangement was adopted, and no further studies of field shape or focusing properties have been made. *Note added in proof:* Field measurements have recently been made by W. D. Warters who finds $n=0.50\pm0.02$ over $r=10.5\pm0.8$ inches.

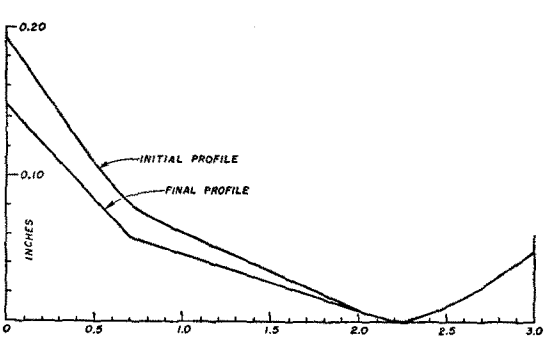

FIG. 2. Profiles of pole faces.

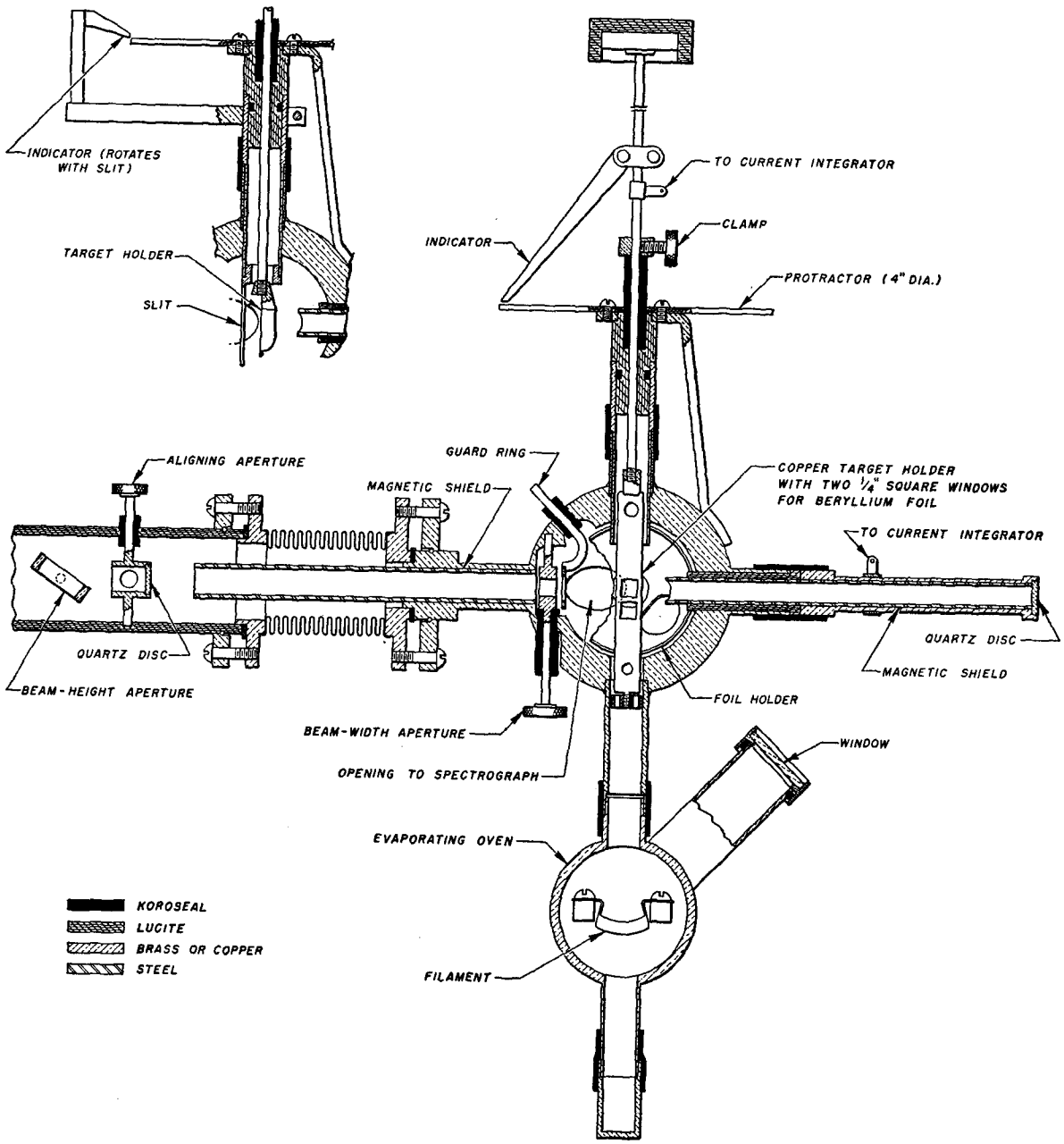

FIG. 3. The target chamber and evaporating oven.

Limitations of Present Design

The maximum field obtainable in the spectrometer with the 15 kw, 120-volt generator proved to be 7000 gauss, corresponding to 2-Mev protons. The most constricted portion of the magnetic circuit was at the intersections of the core with the two yokes. This constriction was eliminated by adding steel pieces as shown by the dashed lines in Fig. 1, but the change increased the peak field in the gap by only about five percent. The difficulty is simply that the leakage flux is very large because of the shape of the magnetic circuit so that the fraction of the total flux which goes through the pole faces is only $\frac{2}{5}$ at low fields and less than $\frac{1}{4}$ at high fields. Hence, the core, which carries all the flux, saturates too soon. It seems probable that a magnet with the present dimensions could be made to bend 4-Mev protons by winding the coils around the pole pieces themselves instead of around the core. It must be remembered, however, that the achievement of the proper inhomogenous field by shaping the pole pieces is dependent on having the permeability of the iron very high, so that the pole pieces cannot be magnetized near to saturation without introducing defocusing effects.

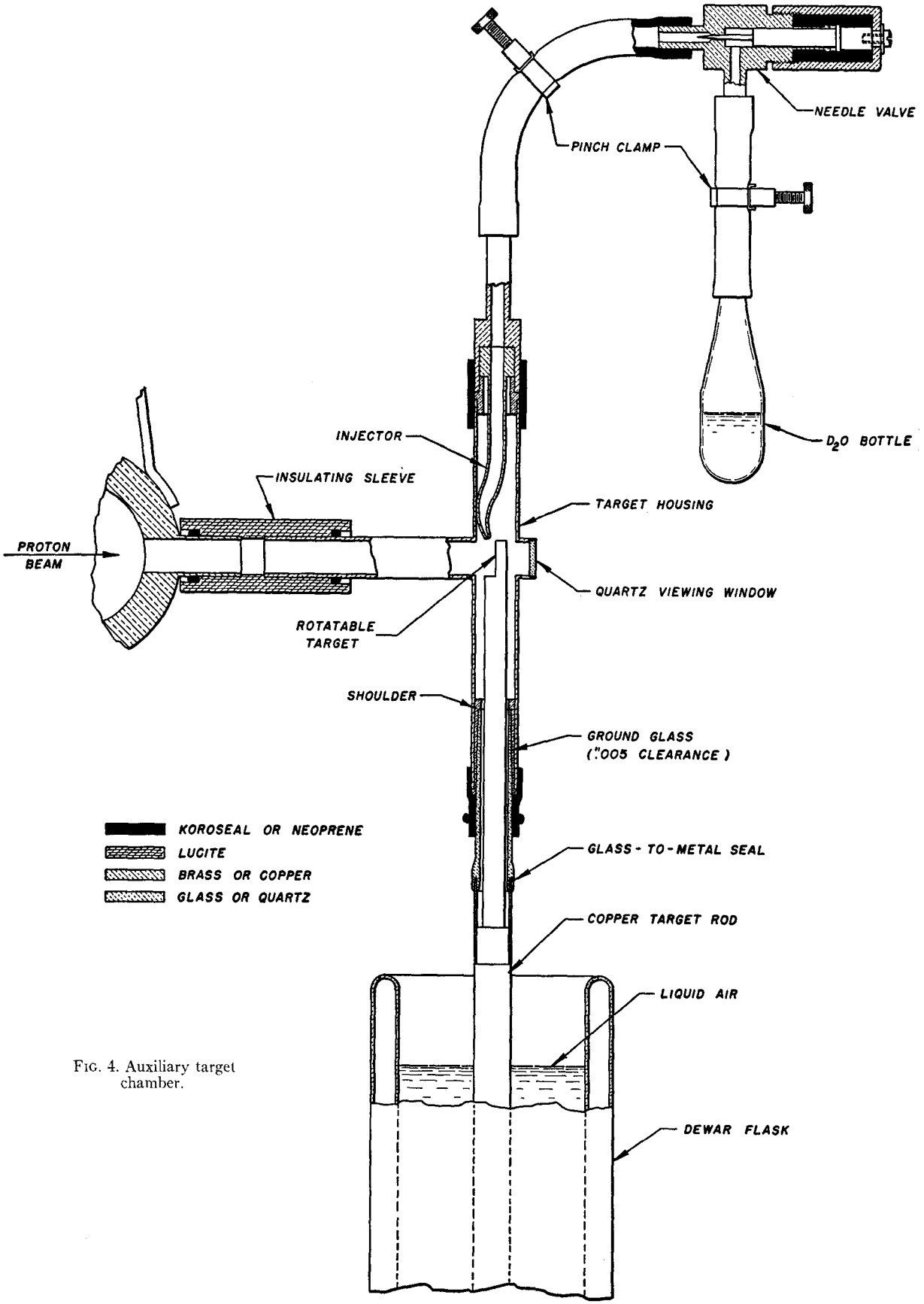

FIG. 4. Auxiliary target chamber.

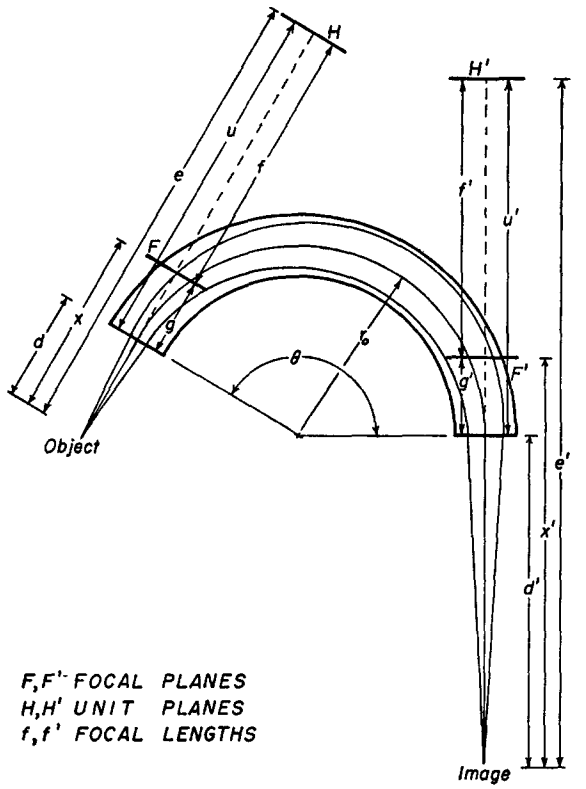

FIG. 5. Constants of the spectrometer as a magnetic lens.

An even more serious difficulty than the inability to focus high energy protons is the presence of the large stray field in the laboratory. It necessitates the magnetic shielding of the incident beam for a distance of several feet and makes the operation of certain instruments (such as photo-multiplier tubes) in the vicinity of the spectrometer very difficult. In spite of the fact that with this spectrometer source and detector are outside of the main field some difficulties remain if the fields outside the gap are not minimized. A 90-degree analyzing magnet[11] and a larger 180-degree double-focusing spectrometer ($r_0=16.0$ in.$=40.6$ cm) have recently been built in this laboratory using "kidney-shaped" coils wound around the pole pieces and having the magnetic circuit completely in iron except for the gap itself. By using flat wire, such a coil can be wound with little difficulty, and the stray field around the magnets is considerably reduced. These instruments will be described in forthcoming publications. The 16-in. double-focusing spectrometer reaches a field of 11,000 gauss (10-Mev alpha-particles and protons) with negligible field outside and has a solid angle of $\sim$0.008 steradian and an observed resolution with a narrow slit ($\frac{1}{32}$ in.) of $p/\delta p=600$.

Fluxmeter

An important auxiliary instrument for use with any magnetic spectrometer having iron in the circuit is, of course, the field measuring device. The fluxmeter designed for this purpose has been previously described.[12] It is mounted so that approximately half the coil is between the pole faces and half in the fringing field. The current necessary to balance the fluxmeter is measured by a Leeds and Northrup Hydrogen Ion Potentiometer Number 7655 and is expressed in millivolts developed across a 1-ohm precision resistor. The readings range from 29 to 100 millivolts and are designated by I in what follows. I is inversely proportional to the magnetic field and thus proportional to the charge/momentum or non-relativistically to the charge/(energy$\times$mass)$^{\frac{1}{2}}$ of the observed particles. The sensitivity is such that the field can be held fixed to 0.05 percent during a run. The pointer is kept on the null mark during a run by manually adjusting the field current in the generator supplying the magnet. The calibration over a period of three years has been reproducible to 0.2 percent.

Target Chamber

The design of the target chamber is shown in Fig. 3. As shown in Fig. 1, it is attached rigidly to the spectrometer through the brass inlet tube and can be moved relative to the proton beam by flexing the sylphon. The alignment of the beam is determined by intercepting it successively at the center of two quartz disks about 13 in. apart. The first disk is mounted in the end of a short length of brass tube pivoted as shown so that the beam can be intercefted by the disk or passed through the $\frac{1}{4}$-in. hole into the target chamber. The other disk is mounted at the outer end of the target tube. For most of its length between these two fixed points, the beam is shielded by steel tubing to minimize curvature of its path in the stray field. The width of beam striking the target is controlled by the defining slit at the left edge of the chamber, which consists of a transverse rectangular opening in a shaft which can be rotated from outside.

The target to be bombarded can be mounted on the end of the second steel magnetic shield, which is beveled so that incident and scattered angles are equal. The tube is perforated so that pressure changes do not damage thin-foil targets and it is insulated from the target chamber by a polystyrene bushing so that it can be used to collect charge for the current integrator. In most experiments the target is mounted on a target holder which can be rotated from outside the vacuum system as shown. A pointer and a fixed protractor indicate the angular position of the target. This target support can also be lowered into a furnace where thin layers of lithium or other materials can be evaporated onto it.

An auxiliary target assembly which can be employed for other types of measurement requiring the proton

[11] D. B. Duncan, Phys. Rev. **76**, 587 (1949).

[12] C. C. Lauritsen and T. Lauritsen, Rev. Sci. Inst. **19**, 916 (1948).

beam without disturbing the spectrometer is shown in Fig. 4. In this particular assembly a heavy ice target was produced by allowing D_2O vapor to enter the target chamber adjacent to the flat face of a copper rod which was kept at liquid air temperatures. For the study of heavy ice targets with the spectrometer, the copper rod and injector system were made so that they could be inserted into the target chamber of Fig. 3 in place of the target holder and furnace shown there. This arrangement for interchanging targets and bombarding positions was found to be a very flexible and convenient one.

For determining the scattering angle, the arrangement shown in the inset in Fig. 3 is used. A brass strip containing a vertical 0.003-in. slit is located so that the slit can be moved on a $\frac{1}{4}$-in. radius about the center of the target foil. Particles scattered by a copper target surface are detected. By rotating the slit so that first the incident beam and then the scattered beam pass through it, an accurate measurement of the scattering angle accepted by the spectrometer can be made.

Detection of Reaction Products

Various types of detectors can of course be used at the focus. The double-focusing spectrometer is advantageous essentially because detectors with small openings can be used with it. An ionization chamber,[13] 1 cm in diameter and 5 mm deep has been used for some experiments. The protons pass through a "Newskin" window of approximately 1-mm air equivalent mounted on a grid, and the ionization chamber reliably counts particles having about 1-mm residual range after traversing the window, so that this set-up is usable with protons of at least 150-kev energy and for alpha-particles with at least 300-kev energy.

For low energy protons a scintillation counter has been used, consisting of a small zinc sulfide screen, a hemispherical reflector and a photo-multiplier.[14] Its chief advantage is its ability to go to very low energies since no window is required, but its lack of dead time is also convenient, obviating the necessity for counting rate corrections. Excellent agreement has been found between absolute yields measured by the two types of counters for energetic particles. The pulse size of the scintillation counts relative to background noise was such that with the bias commonly used to eliminate noise, the counting efficiency was about 90 percent even for low energy particles.

Detection has also been accomplished by photographic plates and end-window proportional counters. The photographic plates are useful for searching for unknown particle groups as they allow use of a very wide slit. The proportional counters are useful in distinguishing protons and alpha-particles of the same energy and $B\rho$ by measurements of the ionization produced in short range intervals.

Source of Incident Particles

The incident beam, protons or deuterons, is obtained from the 1.5-Mev pressure-insulated electrostatic accelerator equipped with a precision electrostatic analyzer.[5] The voltage control is such that the incident proton energy relative to some assumed standard can be fixed to better than 0.2 kev at 1.0 Mev but in order to attain this precision, it is necessary to take considerable care in aligning the beam. This is particularly true since the stray field from the spectrometer magnet deflects the beam appreciably even above the electrostatic analyzer, a distance of more than two meters. The effect is compensated by means of three magnets, two with horizontal fields at right angles above the analyzer and one with a vertical field below the analyzer.

III. THEORETICAL CONSIDERATIONS

We have noted previously that in the axially-symmetric double-focusing spectrometer the conjugate foci are separated from one another by an angle $2\frac{1}{2}\pi = 254.56$ degrees. In the present case, the pole pieces are only 180 degrees in extent, and to a first approximation the foci are found by linear extrapolation beyond the pole pieces of the trajectories inside the field. The spectrometer can then be considered as a "thick" spherical lens and the usual optical theory applied.

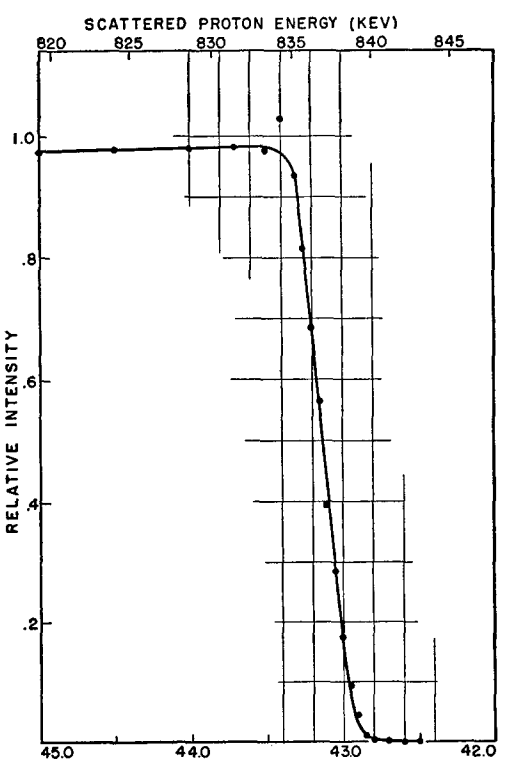

FIG. 6. The elastic scattering of 0.955-Mev protons at 137.8° by a thick copper target.

[13] Thomas, Rubin, Fowler, and Lauritsen, Phys. Rev. **75**, 1612 (1949).

[14] A. Tollestrup, Phys. Rev. **74**, 1561 (1948).

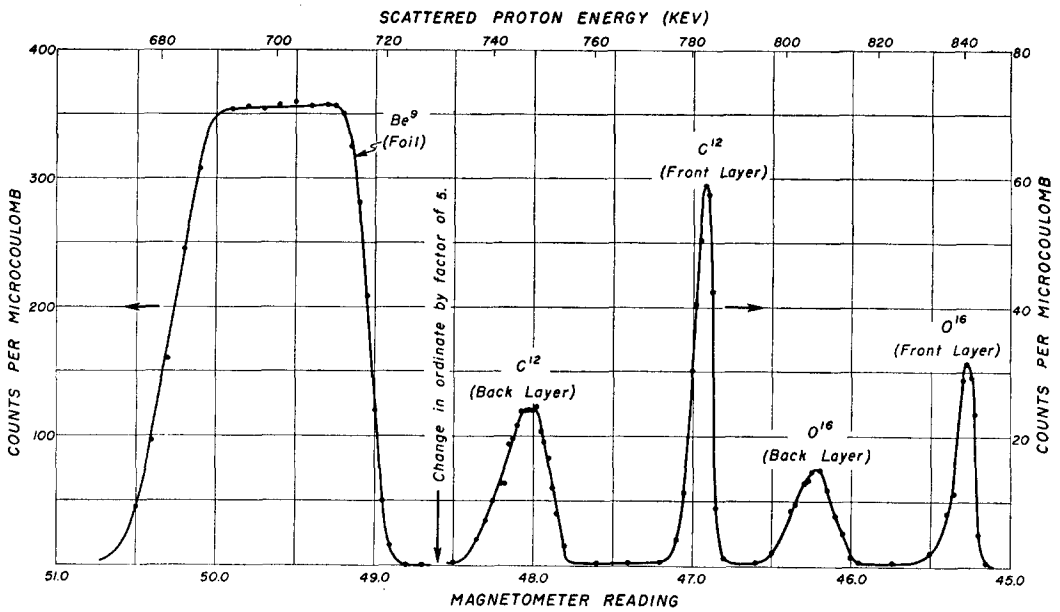

FIG. 7. The distribution in momenta of 1.066-Mev protons elastically scattered at 137.8° by a thin (~18 kev) beryllium foil. Note the sharp peaks arising from carbon and oxygen layers approximately 50 atoms thick on the front and back surfaces of the foil. The scattering from the front layers and from the front surface of the beryllium indicates an over-all momentum resolution of ~500. The effect of straggling in energy loss in the foil on the rear layer and rear surface scattering is noticeable.

The results for any n and any angular extent of the field, θ, have been given by Judd.[10] In what follows we first give the formulas for the anastigmatic case, $n=\frac{1}{2}$ and for any θ. The second expressions are for $\theta=\pi$ while the last expression gives the numerical value for $r_0=26.7$ cm as in the spectrometer described in this paper. The results are illustrated in Fig. 5.

Focal length (i.e. distance between focal planes and unit planes)

$$f=f'=\sqrt{2}r_0\csc\theta/\sqrt{2}=1.78r_0 \quad \text{for} \quad \theta=\pi$$
$$=47.5 \text{ cm} \quad \text{for} \quad r_0=26.7 \text{ cm}. \tag{1}$$

Distance from ends of pole pieces to unit planes (measured inward)

$$u=u'=\sqrt{2}r_0\tan\theta/\sqrt{2}=2.86r_0 \quad \text{for} \quad \theta=\pi$$
$$=76.4 \text{ cm} \quad \text{for} \quad r_0=26.7 \text{ cm}. \tag{2}$$

Distance from ends of pole pieces to focal planes (measured inward)

$$g=g'=-\sqrt{2}r_0\cot\theta/\sqrt{2}=1.08r_0 \quad \text{for} \quad \theta=\pi$$
$$=28.8 \text{ cm} \quad \text{for} \quad r_0=26.7 \text{ cm}. \tag{3}$$

The conjugate focal points, object and image, can be determined from either of the standard relations:

$$1/e+1/e'=1/f \quad \text{or} \quad xx'=f^2, \tag{4}$$

where e and e' are measured from the unit planes and x and x' from the focal planes. However Judd has given the image distance, d', measured out from the pole piece directly in terms of the object distance, d, similarly measured as

$$d'=-\sqrt{2}r_0\tan[\theta/\sqrt{2}+\tan^{-1}d/\sqrt{2}r_0]$$
$$=-\sqrt{2}r_0\tan[127.28°+\tan^{-1}d/\sqrt{2}r_0] \quad \text{for} \quad \theta=\pi$$
$$=-37.8\tan[127.28°+\tan^{-1}d/14.9] \text{ cm}$$
$$\text{for} \quad r_0=26.7 \text{ cm}. \tag{5}$$

We used an object distance, $d=30.5$ cm and found the image distance experimentally to be $d'=8.6$ cm. The calculated image distance is $d'=9.4$ cm in reasonable agreement with the measured value.

The first order anastigmatic image also shows no distortion and the magnification in both the r and z directions is

$$M=\left(\frac{d}{2^{\frac{1}{2}}r_0}\sin\theta/\sqrt{2}-\cos\theta/\sqrt{2}\right)^{-1}$$
$$=\frac{d'}{2^{\frac{1}{2}}r_0}\sin\theta/\sqrt{2}-\cos\theta/\sqrt{2}$$
$$=\left(0.562\frac{d}{r_0}+0.606\right)^{-1}.$$
$$=0.562\frac{d'}{r_0}+0.606 \tag{6}$$

For $d=30.5$ cm, $r_0=26.7$ cm, this gives $M=0.8$. Judd has also calculated the dispersion of the instrument and finds in the general case

$$D=\frac{\delta r}{r_0}\Big/\frac{\delta P}{P_0}=\frac{\delta r}{r_0}\Big/\frac{\delta B}{B_0}=\frac{1+M}{1-n}, \tag{7}$$

where δr is a small increment in the image position measured normal to the optic axis of the spectrometer arising from a change δP in the momentum of the particles injected into the spectrometer or from a change δB in the magnetic induction, B_0, of the spectrometer. We note that $D=2(1+M)$ for the anastigmatic spectrometer as compared with $D=1+M$ for the type with uniform field ($n=0$). For $M=1$ these become $D=4$ and $D=2$ respectively. In the spectrometer described here a magnification of 0.8 was employed for reasons previously given and the dispersion has the value $D=3.6$.

The ultimate resolving power of the instrument can be calculated if the size and shape of the image of a point source formed by the particles emitted in a finite solid angle is known. This in turn depends on higher order calculations and on fringing field effects. Practically we have found no occasion to employ the ultimate resolution as determined by the small image aberrations but have been limited to values of the resolution given by the source and collector sizes dictated by intensity considerations. This resolution in momentum can be computed from the width of the collecting slit, δr_c, by using the expression for D given above

$$R_c=\frac{P_0}{\delta P_c}=\frac{Dr_0}{\delta r_c}=\frac{1+M}{1-n}\left(\frac{r_0}{\delta r_c}\right). \tag{8}$$

In the case described here $R=3.6r_0/\delta r$ For a finite source width, δr_s, a similar expression is obtained by replacing δr_c by $M\delta r_s$ yielding

$$R_s=\frac{P_0}{\delta P_s}=\frac{1+M^{-1}}{1-n}\left(\frac{r_0}{\delta r_s}\right). \tag{9}$$

The apparent spread in momenta, δP_c or δP_s, of particles actually having the same momentum will be indicated in terms of an interval δI_c or δI_s in fluxmeter readings over which counts can be obtained.

For rectangular source and slit the apparent distribution in momentum for monoenergetic particles will be trapezoidal in shape with a width at half-maximum determined by whichever of δP_c or δP_s is the larger and the effective resolution will be determined by the smaller of R_c and R_s. The base of the trapezoid will have a width given by $\delta P_s+\delta P_c$ while the top will have a width given by $|\delta P_s-\delta P_c|$.

For a continuous distribution of particles extending up to a maximum energy as is observed for example when a thick target is used in scattering or reaction experiments, the observed distribution will show the effects of finite resolution near the upper limit. These effects are shown in Fig. 6 which illustrates the distribution in momentum of monoenergetic protons scattered by a thick Cu target. The curve shows a linear portion of finite slope symmetric about the true end point with rounded fillets at each end. If the linear portion be extended from the maximum reading to zero it will be found to cover a momentum range given by δP_c or δP_s, whichever is larger. The corresponding δI_c or δI_s divided into the reading I will give the resolution.

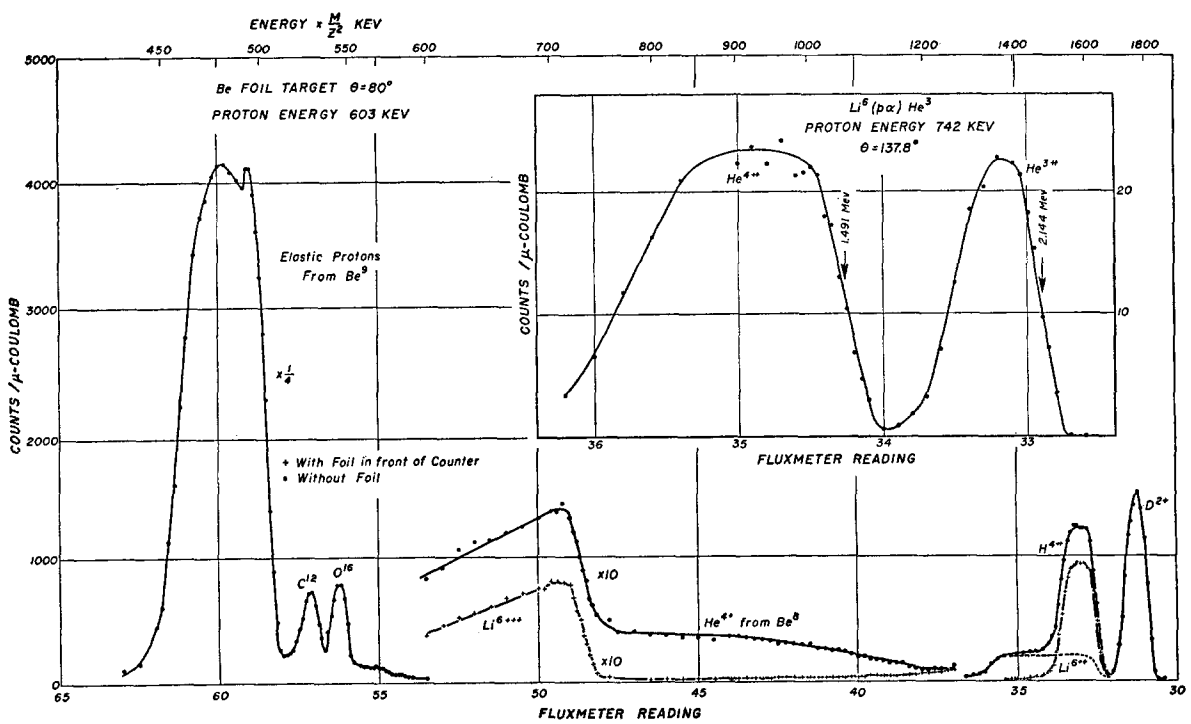

FIG. 8. Momentum analysis of the ions produced in the bombardment of Be^9 and Li^6 by protons.

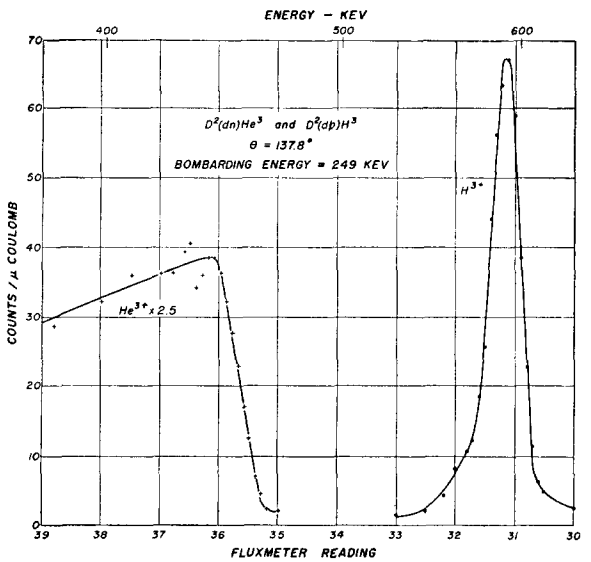

FIG. 9. Momentum analysis of the He^{3+} and H^{3+} produced in the bombardment of deuterons with 249 kev deuterons and with the angle of observation equal to 137.8°.

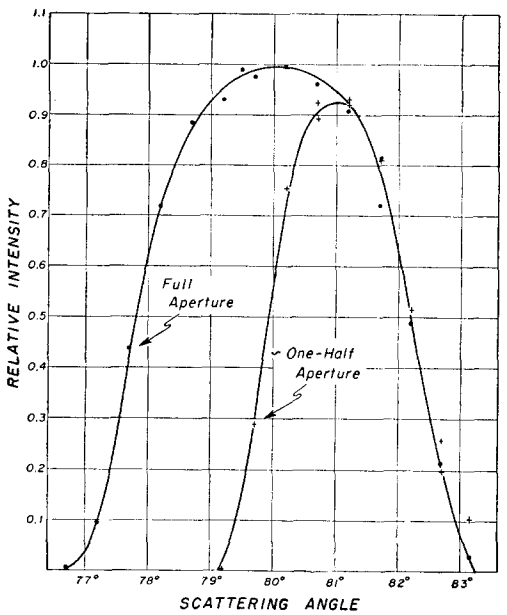

FIG. 10. Distribution in angle of the particles accepted by the spectrometer.

In the use which we have made of the spectrometer δr_c and δr_s have been determined by intensity considerations. The number of counts observed is linear in δr_c as long as the particle spread in energy is greater than that accepted by the spectrometer as is usually the case. The source width is usually determined by the beam width from the electrostatic generator and the useful current depends on the width permitted through the beam slit as long as the focused beam is larger than this slit width. In addition to the apparent spread in energy arising from (1) the source (or bombarding beam) width and (2) the collector width, (3) aberrations and (4) fluctuations in the magnetic field, there are real spreads in energy in the particles entering the spectrometer. These arise from (5) the energy spread in the incident beam (6) the angular extent of the inlet aperture* since the energy of a particle emitted in a nuclear reaction or scattering process depends on the angle of emission, (7) the energy loss in the target of both the incident and outgoing particles and (8) the energy straggling in the target of both particles, and (9) the thermal motion of the target nuclei.

TABLE I. The elastic scattering of protons by several materials. Incident energy = 1.2373 Mev. Angle of scattering = 137.8°. (Relativistic corrections included.)

Scatterer	Calculated energy after scattering E (Mev)	Fluxmeter reading I (mv)	Spectrometer constant for protons C_p
Li	0.7475	48.24	1.7390×10^4
Be	0.8367	45.56	1.7366
C	0.9230	43.39	1.7379
O	0.9931	41.83	1.7382
Cu	1.1704	38.52	1.7376
Mean			1.7379×10^4 ±0.0006

* The finite source size also makes a contribution to the spread in the angle of observation. Its effect must be combined algebraically with (1).

The ultimate line shape can be predicted from a folding of the various contributions listed above into each other. The effect of (7) will depend markedly on whether the outgoing particles emerge into the spectrometer from the same side of the target as the incident particles enter or from the opposite side. The effect will also depend on whether the energy of the particles produced in the nuclear reaction under study decreases as the incident particle energy decreases because of energy loss in the target or whether it increases. For the so-called residual nuclei produced in a nuclear reaction the latter is often the case for angles of observation with the incident beam greater than 90°.

Items (1) to (6) and (9) discussed above make symmetrical contributions to the line shape of a group of particles under observation. Thus for very thin targets for which (7) and (8) can be neglected the observations yield a symmetrical line the midpoint of which corresponds to the momentum (or energy) of the secondary particles produced at the angle corresponding to the mean acceptance angle of the spectrometer by those particles in the incident beam having the mean energy of the beam. Usually for reasons of intensity ideally thin targets cannot be used. In energy determinations if the midpoint of the observed line is employed as a measure of the energy of the secondary particles then a correction must be made for half the energy loss in the target both for the incident and emergent particles. The method of correction will be the same whether the secondary particles emerge from the same side of the target as the primary particles impinge upon or from

TABLE II. The elastic scattering of protons by copper at several energies. Angle of scattering = 137.8°. (Relativistic corrections not included.)

Inc. energy E (Mev)	$\frac{1}{2}$ Scat. energy	Fluxmeter Reading H^+	HH^+	HHH^+	Spectrometer constant for protons calculated from H^+	HH^+	HHH^+
1.3314	1.2603	37.08	52.51	64.34	1.733×10^4	1.737×10^4	1.739×10^4
0.8876	0.8402	45.35	64.30		1.728	1.737	
0.4438	0.4201	64.26			1.735		
Mean						1.735×10^4 ±0.002	

the opposite side if the inclination of the target to the incident and emergent beams is properly taken into account. The contribution to the observed width of the line will of course be markedly different in the two cases. It is clear that other characteristics of the observed thin-target curves such as extrapolated end points can be employed if properly interpreted but we have found it most convenient to use midpoints representing mean energies with appropriate corrections for target energy losses.

Actually in our most accurate energy determinations with the spectrometer we have preferred to employ thick targets. It is then necessary to observe the particles emerging from the surface of the target upon which the incident particles impinge. The measurements yield a step curve (see Fig. 6 for example) which is essentially just the integral of the curve arising from contributions (1) to (6) and (9). The midpoint of the sloping front of the step is taken as the momentum of the secondary particles produced at the mean acceptance angle of the spectrometer by the particles of mean energy in the incident beam. In some cases we have employed semithick targets which do not completely stop the incident particles but which give a spread in energy large compared to that arising from (1) to (6) and (9). In this case we have also used the midpoint of the initial rise just as with thick targets but the accuracy is not as great primarily because of the effect of straggling on the peak reading obtained.

The error in the determination of the energy of a group of particles arises from the following causes with which we also list an estimate of the contribution to the probable error: (1) uncertainty in the fundamental constants, 0.01 percent, (2) uncertainty in the energy of calibration particles, 0.1 percent, (3) uncertainty in fluxmeter setting and line location, 0.2 percent, and (4) uncertainty in the particle path arising mainly from variations in the target or beam position and from saturation effects in the magnetic field, 0.05 percent. The over-all error is slightly over 0.2 percent. In the determination of the Q of a nuclear reaction in addition to (1) the error in the energy of the observed particles, errors arise from (2) uncertainty in the energy of the incident particles, (3) uncertainty in the angle of observation, (4) uncertainty in the masses of the particles involved, (5) uncertainty in the thickness of surface contamination layers on the target, and in some cases, (6) uncertainty in the interpretation of the line structure.

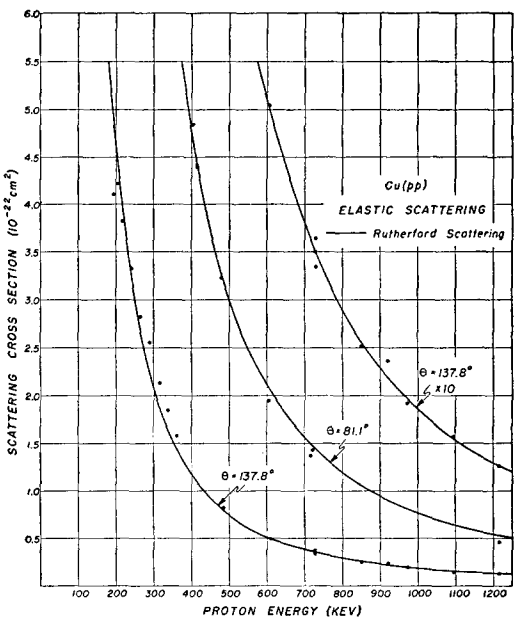

FIG. 11. The cross section for the elastic scattering of protons by copper as a function of energy. The experimental point at $E_p=610$ kev, $\theta=137.8°$ has been fitted to the Rutherford cross section (solid curves) yielding a value for the spectrometer solid angle of 0.0061 steradian.

IV. TESTS AND CALIBRATION

Energy Measurements

The characteristics of the spectrometer have been investigated by scattering protons and deuterons elastically from various targets, particularly gold, copper, oxygen, carbon, beryllium and lithium. A thin beryllium foil* gives a particularly interesting trace as shown in Fig. 7. The foil was thin enough and the bombarding energy high enough so that the scattered protons from beryllium, from carbon and oxygen contamination on the front of the foil, and from similar contamination on the back of the foil are all distinctly separated in energy. The separation occurs because of the differing amounts of recoil energy imparted to nuclei of different mass and because of the energy loss of incident and scattered protons in the beryllium. The high resolution in momentum ($\sim$500) arises from the fact that $\delta r_c=\delta r_s=0.1$ cm in these measurements. Figure 8 shows an example of what happens with a lower bombarding voltage and a wider exit slit (0.8 cm). Here the peak from the front oxygen layer is clearly apparent while the peaks from the rear oxygen layer and the front carbon layer occur at the same reading. The peak from the rear carbon layer lies atop the beryllium peak, which therefore appears to have an unusual shape. Such effects must

* This foil and others were very kindly supplied to us by Dr. Bradner of the University of California. The technique of preparing them is discussed in Rev. Sci. Inst. **19**, 662 (1948).

be taken into consideration in making accurate energy measurements.

Figure 8 also shows the nuclear reaction products obtained in the bombardment of Be^9 and Li^6 by protons. The reactions are $Be^9(p, \alpha)Li^6$, $Be^9(p, d)Be^8$, and $Li^6(p, \alpha)He^3$. The singly ionized deuterons, doubly ionized alpha-particles, doubly ionized He^3 and both the doubly ionized and the triply ionized Li^6 give definite peaks. The Be^8 produced in the second reaction breaks into two alpha-particles with random directions in the moving center of mass system yielding the continuous distribution of alpha-particles in the laboratory system which is also clearly indicated. These results have been analyzed in a previous publication.[15] Another set of measurements which have also been previously described[1] are shown in Fig. 9. Here the residual nuclei from $D(d, p)H^3$ and $D(d, n)He^3$ have been measured by bombarding heavy ice targets with deuterons. In these measurements considerable analysis was necessary to properly interpret the "thin" target curve for H^3 and the "thick" target curve for He^3 obtained using the same target and the analysis carried out along the lines discussed above is given in detail in the reference.

The results obtained by elastically scattering protons or deuterons of known energy at a known angle from various targets has been used to calibrate the momentum (or energy) scale of the fluxmeter. The energy of the incident particles is determined by means of the electrostatic analyzer calibrated at the strong gamma-resonance in $F^{19}(p, \alpha'\gamma)$ at 873.5 ± 0.9 kev.[16] The angle of scattering was determined by means of observations with the rotating slit described previously. A record of the data taken with the slit and two settings of the entrance aperture is shown in Fig. 10. With the aperture stop completely open the mean scattering angle seen by the spectrometer as set up in this particular experiment is 80° with some particles being accepted up to 3° on either side of this. To improve the resolution some data has been taken with the aperture stop partially closed. It will be noted in Fig. 10 that for this setting the mean angle is 81° with a spread of slightly less than 2° on either side.

In Table I we present the results of the elastic scattering of 1.2373-Mev protons at 137.8° by Li, Be, C, O, and Cu. Column 2 lists the energies after scattering (E) calculated using the conservation laws of energy and momentum. Small relativistic corrections have been made. These arise in the energy determination in the analyzer and in the calculation of the energy after scattering. Column 3 lists the fluxmeter readings in millivolts (I). In column 4 are listed values of the spectrometer constant for protons as calculated from:

$$C_p = I^2E[1+(E/2M_pc^2)],$$

where M_p is the mass of the proton appearing in the second terms in brackets which is a small relativistic correction. The results for the various determinations of C_p indicate the high precision possible with the spectrometer. The average value from these determinations is $C_p = 1.738 \times 10^4$ for E in Mev and I in millivolts. This value for C_p holds only for protons. The constant for any other ion of charge Z and mass M can be obtained by multiplying C_p by M_pZ^2/MZ_p^2 or by Z^2/M for M in proton mass units.

In passing it is worth noting that the observation of elastic scattering peaks with spectrometers of high resolution is an excellent method for determining the nuclear composition of thin layers of unknown materials. Since the Rutherford scattering increases as the square of the nuclear charge the method is especially sensitive in detecting minute quantities of heavy nuclei. Very high resolution (10^4) and very thin targets (<100 ev) are necessary to separate the heavy nuclei even at large angles of scattering.

By using the hydrogen ion beams of masses one, two, and three with a constant setting on the electrostatic analyzer for the incident protons, one can check the linearity of the magnetic fluxmeter and establish the precision with which measurements can be made with the spectrometer. Similarly with fixed fluxmeter settings one can check the linearity of the analyzer. In Table II we give readings for three energies in the ratio 3,2,1 taken with copper as the scattering material. The calculated values for C_p are also given.

Small relativistic corrections and corrections for the electrons carried by ions of mass two and three have not been included. Even without these corrections the results show that the over-all combination of electrostatic analyzer for incident particles and of magnetic analyzer for outgoing particles gives consistent results within a probable error of 0.1 percent.

Resolution and Line Width

Very thin targets or infinitely thick ones can be used in elastic scattering experiments to yield a measure of the line width arising from source and exit slit size. In the former case the energy losses can of course be neglected while in the latter case the slope of the rise to the maximum reading can be employed to calculate the line width neglecting target losses. Using an exit slit $\delta r_c = 0.8$ cm and an entrance slit $\delta r_s = 0.2$ cm so that δr_c determines the resolution we have made careful measurements using thick Cu targets of the rise in the scattering curve. We find $\delta I/I = 0.0081$, 0.0075, and 0.0078 in measurements at 1240, 992, and 744 kev yielding an average value 0.0078 and a resolution $R = 128$. Our expression for R is the resolution in particle momenta. Since energy is proportional to momentum squared, we have $E/\delta E = \frac{1}{2}P/\delta P = \frac{1}{2}R = 64$. If we substitute $M = 0.8$, $n = 0.5$, $\delta r_c = 0.8$ cm, $r_0 = 26.7$ cm into expression 8, we obtain $R = 122$ in good agreement with the observed value. Simple calculations indicate that the spread in energy in the incident beam and

[15] Tollestrup, Fowler, and Lauritsen, Phys. Rev. **76**, 428 (1949).
[16] Herb, Snowdon, and Sala, Phys. Rev. **75**, 246 (1949).

in the scattered particles over the entrance aperture contribute values of $\delta I/I \sim 0.001$ and merely increase the fillets on the observed curves. The widths of the carbon and oxygen peaks shown in Fig. 7 which were obtained using 0.1-cm entrance and exit slits indicate $R \approx 500$ while the calculated value is $R \approx 1000$. In this case the contribution to line width from the angular extent of the aperture is not negligible.

We have made no attempt to measure the ultimate inherent resolution of the spectrometer. However the image size due to aberrations of a point source of protons as described above was visually estimated to be of the order of 0.1 cm in size. Substitution in 8 above yields $R \sim 1000$. There is reason to believe that the recognition of detail even to better than one part in a thousand in momentum is possible with sufficiently intense sources.

Solid Angle

The solid angle of acceptance of the spectrometer can be determined by measuring the yield of elastic scattering from a substance such as copper. The measurements we have made are illustrated in Fig. 11 and show a $1/E^2$ dependence over the entire energy range showing that there are no anomalies in the Rutherford scattering. With a thick target the yield is of course proportional to the Rutherford cross section and to the target thickness in which the over-all losses are just enough to fill the exit slit of the spectrometer. This involves the instrument resolution and the stopping cross section for protons in Cu. The data shown in Fig. 11, using Mano's stopping power for Cu, are consistent with a value for $\Omega = 0.0061$ steradian or $\sim 1/2000$ of the sphere. Using the formula for Ω given by Judd we calculate $\Omega = 0.008$ steradian from the *maximum* available cross section of the spectrometer vacuum tank. That the experimental result is slightly smaller than the value so calculated is not surprising in view of the fact that other stops in the system probably determine the solid angle.

Yield Measurements

In a future paper we intend to discuss the use of the spectrometer in the measurement of the intensity of particles produced in a nuclear reaction. We note at this point that the number of counts observed in the detector, N, for a given yield, y, of particles produced at the target per unit momentum interval per 4π steradians of solid angle, is

$$N = y(\Omega \delta P_c/4\pi),$$

where δP_c is the momentum interval corresponding to the collector slit width and Ω is the solid angle through which particles leaving the source can traverse the spectrometer and enter the detector. In terms of $R_c = P/\delta P_c$ we have

$$N = y(\Omega P/4\pi R_c).$$

We emphasize that it is the resolution, R_c, appropriate to the collector size which appears explicitly in this expression and not the resolution, R_s, appropriate to the source, nor the resolution, R_a, arising from aberrations such as spherical aberration. It is true that in certain cases y may depend on the area of the source, as for radioactive deposits with a limiting surface activity or for targets which can be bombarded only by beams of limited concentration. Also, of course, Ω and R_a are intimately related and numerous papers have been written proposing methods for obtaining small aberrations and thus high resolution R_a for a given solid angle. In the last analysis it must be noted that it is R_c which appears in N and there are many practical cases in which to obtain sufficient counts for the maximum solid angle in the available magnetic field volume, one must reduce R_c to a value considerably below the ultimate value R_a so that the observed resolution is of the order of R_c and not of R_a. In these cases many other considerations may dictate a choice of design parameters which do not yield a high value of R_a but other desirable features such as low power consumption, ease and simplicity of construction, and so forth. Only in those cases where R_c can be matched to R_a will the practical resolution and the ultimate be approximately equal.

For the spectrometer discussed in this paper we have found

$$\frac{N}{yP} = \frac{\Omega}{4\pi R_c} = 3.80 \times 10^{-6}$$

or

$$R_c/\Omega = 21{,}000,$$

where $R_c = 128$ for the 0.8-cm collector slit which was employed in most measurements and $\Omega = 0.0061$ steradian for the full aperture. If R_c had been matched to the ultimate resolution $R_a \sim 1000$, a result eight times smaller would have been obtained which would have been impractical for applications involving nuclear processes of low probability.

In determining yields and cross sections in nuclear reactions from observed counting rates, we have

$$y(I) = \frac{4\pi R_c}{q\Omega_c} \frac{N(I)}{I} \times 1.6 \times 10^{-13}$$

$$= \frac{2R_c}{q\Omega_c} \frac{N(I)}{I} \times 10^{-12}$$

where $y(I)$ is the yield per incident singly charged particle per 4π steradians in the center-of-mass system per unit interval on the fluxmeter scale and $N(I)$ is the number of counts observed at the fluxmeter reading I when q microcoulombs strike the target. The equivalent solid angle Ω_c, in the center-of-mass system, can be calculated in a straightforward manner from Ω. *For thin targets* one can integrate over the total area under

the peak corresponding to a given group of particles and obtains

$$Y=\int y(I)dI=\frac{2R_c}{q\Omega_c}\int\frac{N(I)}{I}dI\times 10^{-12}$$

which is the yield in disintegrations per incident particle per 4π steradians appropriate to the target thickness and angle of observation employed. The cross section is then given by thin target measurements as

$$\sigma=Y/nt=Y\epsilon_1/\xi_1$$
$$=\frac{2R_c\epsilon_1}{q\Omega_c\xi_1}\int\frac{N(I)}{I}dI \quad \text{millibarns},$$

where n=disintegrable nuclei per cc in the target, t=target thickness parallel to the incident beam in cm, ξ_1=energy loss of incident particles in target in ev, and ϵ_1=stopping cross section[15] in 10^{-15} ev-cm^2 for the incident particles per disintegrable nucleus in the target molecules. *For targets thick* enough that the energy spread of the outgoing particles exceeds the total energy spread from all other causes including in particular the energy interval accepted by the spectrometer collecting slit, it is often convenient to use the maximum reading over the flat portion of the observed curve of counts *versus* spectrometer setting. Similarly for very thick targets it is convenient to use the maximum reading obtained after the initial rise. In both cases if $N_{\max}$ is this maximum reading for q microcoulombs

$$Y=2N_{\max}/q\Omega_c\times 10^{-12},$$

where Y is now the yield in disintegrations per incident particle per 4π steradians appropriate to the target thickness which just gives a spread in energy of the outgoing particles equal to that accepted by the spectrometer collecting slit. A simple calculation gives this thickness in energy units as

$$\xi_1=\frac{\epsilon_1\delta E_2}{|\epsilon_1(\partial E_2/\partial E_1)+\epsilon_2(\cos\theta_1/\cos\theta_2)|}$$
$$=\frac{2\epsilon_1 E_2}{R_c|\epsilon_1(\partial E_2/\partial E_1)+\epsilon_2(\cos\theta_1/\cos\theta_2)|},$$

[15] Livingston and Bethe, Rev. Mod. Phys. **9**, 270 (1937).

where ϵ_2=stopping cross section in 10^{-15} ev-cm^2 for the outgoing particles per disintegrable nucleus in the target molecules. E_2=energy of outgoing particles in electron-volts. θ_1=angle of incident beam measured from the normal to the target on the side of the incident beam. θ_2=angle of outgoing particles measured from the normal to the target on the side of the incident beam. $\partial E_2/\partial E_1$=variation in energy of outgoing particles with that of the incident particles calculated from the expression $E_2=E_2(E_1, \theta, Q)$ given by the application of the usual conservation laws. The cross section is thus given by thick target measurements as

$$\sigma=\frac{N_{\max}R_c}{q\Omega_c E_2}\left|\epsilon_1\frac{\partial E_2}{\partial E_1}+\epsilon_2\frac{\cos\theta_1}{\cos\theta_2}\right| \quad \text{millibarns}.$$

Great care must be observed in using this expression if $\partial E_2/\partial E_1<0$ as is often the case for residual nuclei or if $\cos\theta_1/\cos\theta_2<0$ as in transmission experiments. In either case straggling in energy loss of the outgoing particles may make a large contribution to their observed spread in energy and a calculation taking this into account must be made. In most of our experiments observations have been made on the light particles emitted in a nuclear reaction for which $\partial E_2/\partial E_1>0$. The one exception has been discussed in detail previously.[1] In addition, in most of our experiments we have observed on the side of the target on which the bombarding particles were incident so that $\cos\theta_1/\cos\theta_2>0$. The reason for this is that this choice is convenient for large angles of detection with the incident beam. At these angles Rutherford scattering of the incident particles is small and not considerably greater than nuclear processes as it is at forward angles. This reduces the interference from the scattered incident particles. Observations in this manner are of course the only method for targets so thick that the particles cannot emerge from the side opposite to the incident beam.

In conclusion we wish to thank Professor R. F. Christy and Dr. D. L. Judd for many illuminating discussions of this paper.

This work was assisted by the joint program of the ONR and AEC.